Coupled electron-nuclear spin dynamics in quantum dots: A graded box model approach

M. Yu. Petrov,[1,*] G. G. Kozlov,[1] I. V. Ignatiev,[1,2] R. V. Cherbunin,[1,2] D. R. Yakovlev,[2,3] and M. Bayer[2]
[1]*Physics Department, St. Petersburg State University, St. Petersburg 198504, Russia*
[2]*Experimentelle Physik 2, Technische Universität Dortmund, D-44227 Dortmund, Germany*
[3]*A. F. Ioffe Physico-Technical Institute, Russian Academy of Sciences, St. Petersburg 194021, Russia*
(Received 27 April 2009; revised manuscript received 14 August 2009; published 17 September 2009)

The dynamics of electron and nuclear spin polarization in an ensemble of singly negatively charged quantum dots subject to optical excitation is theoretically studied using a graded box model, in which the electron density is approximated by a sequence of steps. The model is numerically implemented for a limited number of nuclei (up to $N=192$) with spins $I=1/2$ or $I=3/2$. The polarization dynamics is found to depend strongly on the polarized excitation protocol. For excitation by periodic laser pulses, the electron-nuclear spin dynamics evolves coherently and gives rise to a recurrence effect in the electron spin dynamics as well as to a decelerated nuclear polarization. The validity of the model is justified by comparison with experimental data on the electron spin polarization in (In,Ga)As/GaAs quantum dots.

DOI: 10.1103/PhysRevB.80.125318 PACS number(s): 72.25.Fe, 03.67.Pp, 71.70.Jp, 78.67.Hc

I. INTRODUCTION

The spin physics in semiconductor nanostructures has been intensely studied during recent years, for reasons of fundamental interest and application potential.[1–3] In singly charged quantum dots (QDs) the electron spin is strongly coupled to the nuclear spins because of the enhanced hyperfine interaction compared to systems of higher dimensionality.[4] The interaction with randomly oriented nuclear spins is the main electron-spin decoherence mechanism in QDs.[5,6] To achieve a long-term electron-spin memory this relaxation mechanism can be suppressed by an external magnetic field[7] or by dynamical nuclear spin polarization (DNSP)[8] as both mechanisms stabilize the electron spin along a preferential direction. Owing to this, the DNSP dynamics in QDs has been an active field of research.

The dynamics of electron spin coupled to nuclear spins by hyperfine-mediated interaction has been analyzed theoretically by many groups.[9–13] The authors of these papers examined the electron-spin evolution after a single event of spin orientation. However, the obtained results contain no information about the DNSP dynamics, which can be created only by an extended sequence of such orientation events. A theoretical analysis of DNSP dynamics in QDs has been done in Refs. 14 and 15. In particular, Christ *et al.* (Ref. 15) considered the problem of nuclear polarization in the approximation of short correlation time (which is the time of coherent evolution of the electron-nuclear spin system). However, these conditions do not match those in optical experiments with QDs containing resident electrons where the correlation time is long.[16]

Due to the large number of nuclei coupling to a QD electron spin, $N\propto 10^5$, an exact solution of the quantum mechanical problem of electron-nuclear spin dynamics is impossible, both analytically and numerically. To obtain insight into the underlying physics simplified but exactly solvable models, which are reasonable approximations of the complex dynamics, are required. Exact solution of the quantum mechanical problem of nuclear spin dynamics for an arbitrarily large number of nuclei can be obtained by the so called "box model,"[17,18] which assumes an uniform distribution of the electron density over all nuclei within the QD. The main drawback of the box model is that it cannot explain the high values of DNSP observed experimentally.[19,20] Calculations of the spin dynamics by direct diagonalization of the corresponding Hamiltonian for a small ($N\propto 10$) number of nuclei[14] show that taking into account the inhomogeneity of electron density in a QD considerably increases the upper limit of nuclear polarization.

In this paper, we propose a modification of the box model, the "graded box model" in which the spatial variation in the hyperfine interaction is taken into account in a simple and transparent way. Using this model we calculate the dynamics of the electron-nuclear spin system in a QD containing a resident electron with a wave function spread over a limited number of nuclei with spins $I=1/2$ or $I=3/2$. We consider the electron-nuclear spin dynamics in the time range when the hyperfine interaction plays the main role. This range is considerably shorter than the time of irreversible electron and nuclear spin relaxation processes via interaction with phonons,[21–23] nuclear spin dipole-dipole interaction,[24] etc. Therefore, no irreversible spin-relaxation processes are taken into account. We consider the spin dynamics initiated by optical pumping for both periodic and aperiodic pulses. These two cases mimic excitation by pulsed periodic and continuous-wave laser radiation, respectively. To validate the model, we qualitatively compare the results with experimental measurements of the spin dynamics in an (In,Ga)As/GaAs QD ensemble.

II. MODEL

First, we describe the basic assumptions of the graded box model. The Fermi contact interaction, which couples the electron spin $\hat{\mathbf{S}}$ with nuclei spins $\hat{\mathbf{I}}_j$, is described in first order perturbation theory by the Hamiltonian[6]

$$\hat{\mathcal{H}}_{\mathrm{hf}} = v_0 \sum_j A^j |\psi(\mathbf{R}_j)|^2 (\hat{\mathbf{S}} \cdot \hat{\mathbf{I}}_j), \tag{1}$$

where v_0 is the unit-cell volume, A_j is the hyperfine coupling constant, and $\psi(\mathbf{R}_j)$ is the electron envelope wave function at

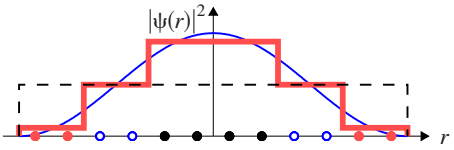

FIG. 1. (Color online) Approximation of the cosine-squared electron density (thin solid line) by a sequence of step functions for 12 nuclei arranged in three equivalent nuclei groups (thick solid line). The nuclei belonging to one group are represented by a particular type of circles. The box model approximation where all nuclei are equivalent is indicated by the dashed line.

nuclear site $\mathbf{R}_j$. The sum in Eq. (1) runs over all nuclei in the QD electron localization volume.

The smooth electron-density distribution $|\psi(\mathbf{r})|^2$ is approximated by a function consisting of n steps from the edge toward the center. Within each step the electron distribution is given by $|\psi_k|^2$, $k=1,\ldots,n$, such that: $0=|\psi_0|^2<|\psi_1|^2<\ldots<|\psi_n|^2=|\psi|^2_{\max}$ (see Fig. 1). The nuclei within the step $|\psi_{k-1}|^2<|\psi(\mathbf{R}_j)|^2<|\psi_k|^2$ belong to the kth group for which the coupling to the electron spin is constant. In this way, we obtain n groups of equivalent nuclei. Then, averaged hyperfine coupling constants $\mathcal{A}^{(k)}$ are introduced for each group of nuclei by: $v_0\Sigma_{j\in(k)}A_j|\psi(\mathbf{R}_j)|^2/\mathcal{N}_k=\mathcal{A}^{(k)}|\psi_k|^2$, where the sum goes over all $\mathcal{N}_k$ nuclei in the kth group.[25] With the total nuclear spin for each group, $\hat{\mathcal{I}}^{(k)}=\Sigma_{j\in(k)}\hat{\mathbf{I}}_j$, $k=1,\ldots,n$, the Hamiltonian (1) can be rewritten in the form

$$\hat{\mathcal{H}}=\sum_{k=1}^{n}\mathcal{A}^{(k)}|\psi_k|^2\left[\hat{S}_z\hat{\mathcal{I}}_z^{(k)}+\frac{1}{2}(\hat{S}_+\hat{\mathcal{I}}_-^{(k)}+\hat{S}_-\hat{\mathcal{I}}_+^{(k)})\right], \qquad (2)$$

where $\hat{S}_\pm$ and $\hat{\mathcal{I}}_\pm^{(k)}$ are rising and lowering operators which increase and decrease the spin z projections $\hat{S}_z$ and $\hat{\mathcal{I}}_z^{(k)}$, respectively. Obviously, the accuracy of this approximation is improved with increasing number of equivalent-nuclei groups. The model with just one group gives the box model.

To calculate the DNSP dynamics in an ensemble of identical QDs, we use the density-matrix formalism. In the initial state, all nuclei are assumed to be unpolarized (the high-temperature state) so that the nuclear density matrix is $\rho_n=\mathbb{1}/G$ with the total number of nuclear spin states G and the unity matrix $\mathbb{1}$. At moments $t=T_m$, $m=0,1,2,\ldots$, short laser pump-pulses polarize the electron spin. These well-defined polarization states are accounted for in the electron-density matrix by $\rho_e=\left[\begin{smallmatrix}\cos^2\phi_m & 0\\ 0 & \sin^2\phi_m\end{smallmatrix}\right]$, where the degree of polarization is determined by the angles ϕ_m. For circularly polarized excitation, either $\phi_m=0$ or $\phi_m=\pi/2$ depending on the helicity of polarization. The laser pulses are assumed to be so short that the nuclear-spin state is left unchanged during their action, so that ρ_n is continuous at each moment T_m. This state can be extracted from the total electron-nuclear density matrix ρ right before T_m by partial averaging over the electron-spin states: $\rho_n(T_m)=\langle\rho(T_m-0)\rangle_e$. By doing so, the total density matrix describing the system immediately after the mth electron-spin orientation event is

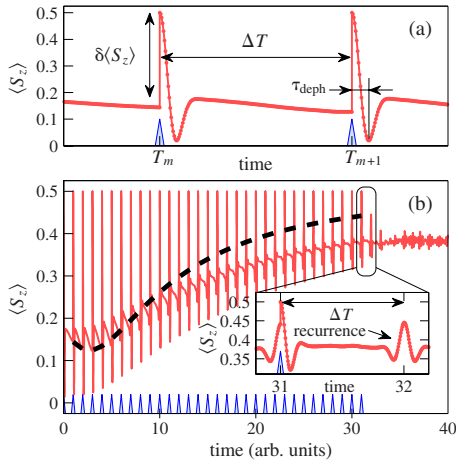

FIG. 2. (Color online) (a) Dynamics of average electron-spin between subsequent orientation events at times indicated by the triangles. The calculations are made for a QD containing 12 nuclei with spins $I=3/2$ and the wave-function approximated by three steps. (b) Electron-spin dynamics for periodic pump excitation. Dashed line shows $\langle S_z\rangle$ just before electron-spin orientation. Inset gives zoom of this dependence after the last excitation pulse.

$$\rho(T_m+0)=\langle\rho(T_m-0)\rangle_e\otimes\begin{bmatrix}\cos^2\phi_m & 0\\ 0 & \sin^2\phi_m\end{bmatrix}. \qquad (3)$$

Between the moments of electron-spin orientation, the electron-nuclear system evolves coherently according to the von Neumann equation,[26] so that

$$\rho(T_m+\tau)=\exp[-i\hbar\hat{\mathcal{H}}\tau]\rho(T_m+0)\exp[+i\hbar\hat{\mathcal{H}}\tau], \qquad (4)$$

where $\hbar$ is the reduced Planck constant and $\hat{\mathcal{H}}$ is given by Eq. (2).

From solution of Eqs. (3) and (4) we obtain the electron-nuclear spin dynamics. An advantage of the graded box model is that the matrix representation of the Hamiltonian has block-diagonal form using the basis functions $|\Upsilon\rangle=|S_z,J_1,L_1,\ldots,J_n,L_n,\beta\rangle$ where $S_z=\pm1/2$ is the electron-spin projection along z, J_k and L_k are the quantum numbers of the total nuclear momentum and its z projection for the kth nuclei group, respectively, and β is the set of other quantum numbers needed for specifying the nuclear state. The equations of motion for the density matrix have been solved numerically by diagonalizing each block of the Hamiltonian matrix using the block-tridiagonal divide-and-conquer algorithm[27] [see Appendix for details].

III. ELECTRON-NUCLEAR SPIN DYNAMICS UNDER EXCITATION WITH CONSTANT HELICITY

A suitable tool for testing the nuclear-spin state is detection of the electron-spin polarization degree,[24] i.e., the observable is $\langle S_z\rangle=\mathrm{tr}[\rho\cdot\hat{S}_z]$. We consider the electron-nuclear spin dynamics for periodic circularly polarized laser pulses of fixed helicity. The corresponding time evolution of the electron spin polarization is shown in Fig. 2.

Figure 2(a) shows the electron-spin dynamics at the initial stage of the excitation protocol. The overall behavior agrees

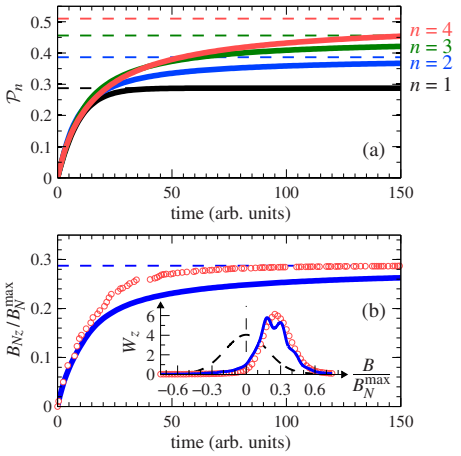

FIG. 3. (Color online) (a) Dynamics of DNSP for 24 nuclei with $I=1/2$ but different numbers of nuclei groups. The DNSP steady-state values are shown by the dashed lines. (b) Dynamics of DNSP calculated for 48 nuclei in 2 nuclei groups for periodic (solid line) and random (circles) excitation protocols. The inset shows the statistics of NSF without pumping (dashed line) and for periodic (solid line) and aperiodic (circles) pumping.

well with the one obtained by Merkulov *et al.* (Ref. 6) within a phenomenological approach. After the orientation event, at T_m, the electron spin rapidly relaxes toward some minimum and reaches its steady state value of $\langle S_z\rangle_{ss}=S_0/3$ where $S_0=1/2$ is the initial value of electron-spin polarization. This evolution is due to the electron-spin precession in the effective magnetic field of nuclear spin fluctuations (NSF).[6] For modeling the electron-nuclear spin dynamics we have chosen the pump-repetition period, $\Delta T=T_{m+1}-T_m$, to be ten times longer than the electron-spin dephasing time, τ_{deph}, which is about a nanosecond (see Refs. 6 and 7). This setting is typical for experimental conditions for pulsed optical pumping the electron and nuclear spins in self-assembled QDs.[28] The arb. unit of the time axis in the figures equals to the repetition period of laser excitation ΔT.

The coupled electron-nuclear motion is interrupted by the next electron-spin orientation event, at which the angular momentum gained from the previous pump-pulse is saved in the nuclear-spin system. The increased DNSP affects the electron spin as an effective magnetic field directed along the z axis. Therefore, the electron spin becomes less depolarized with each subsequent pulse [see Fig. 2(b)]. If the pump polarization protocol is periodic, also a recurrence effect appears in the coherent electron-nuclear spin dynamics as shown in the inset of Fig. 2(b). We will discuss this effect in detail below.

According to the excitation protocol, the DNSP increases with every pump-pulse. To illustrate this we have calculated the DNSP degree which is the ratio of the average nuclear spin z projection to its maximum value: $\mathcal{P}_n=\langle \mathcal{I}_z\rangle/(NI)$, where $\langle \mathcal{I}_z\rangle=\Sigma_{k=1}^{n}\Sigma_{\mathcal{J}} w_{\mathcal{J}}\,\mathrm{tr}[\rho_{\mathcal{J}}\cdot\hat{\mathcal{I}}_z^{(k)}]$. Here, $\rho_{\mathcal{J}}$ is the density matrix block characterized by the set of quantum numbers $\mathcal{J}=\{J_1,J_2,\ldots,J_n\}$ and $w_{\mathcal{J}}=\Pi_{k=1}^{n}\Gamma_{\mathcal{N}_k}(\mathcal{I}^{(k)})$ is the probability for reaching a state with a particular $\mathcal{J}$. The functions $\Gamma_{\mathcal{N}_k}(\mathcal{I}^{(k)})$ are the numbers of possible realizations of an angular momentum $\mathcal{I}^{(k)}$, obtained by summing $\mathcal{N}_k$ elementary spins I according to a procedure described in Ref. 18. For spins $I=1/2$ this results in:

$$\Gamma_{\mathcal{N}}(\mathcal{I})=C_{\mathcal{N}}^{\mathcal{N}/2-\mathcal{I}}-C_{\mathcal{N}}^{\mathcal{N}/2-\mathcal{I}-1}, \tag{5a}$$

and for spins $I=3/2$:

$$\Gamma_{\mathcal{N}}(\mathcal{I})=\sum_{k,m=0}^{\mathcal{N}} C_{\mathcal{N}}^{k}C_{\mathcal{N}}^{m}\cdot[\delta(2m+k-3\mathcal{N}/2+\mathcal{I}) - \delta(2m+k-3\mathcal{N}/2+\mathcal{I}+1)] \tag{5b}$$

where $C_{\mathcal{N}}^{k}$ is the binomial coefficient and $\delta[n]$ is the Kronecker delta.

The DNSP dynamics calculated for a periodic excitation protocol ($\phi_m=0$ and $T_{m+1}-T_m\equiv\Delta T$ for all m) is shown for different numbers of equivalent-nuclear groups in Fig. 3(a).[29] The DNSP time dependence consists of fast and slow stages. Similar dependencies obtained in the frame of different approximate models have already been reported by Christ *et al.* (Ref. 15). At the initial stage of polarization, the different time evolutions of the DNSP degree closely follow each other and then saturate at their steady-state values, $\mathcal{P}_n^{ss}$, which differ for the different models. The steady-state values correspond to total polarization in each density matrix block $\rho_{\mathcal{J}}$ and can be estimated by $\mathcal{P}_n^{ss}=\mathcal{P}_1^{ss}(N)\sqrt{n}$ where $\mathcal{P}_1^{ss}(N)$ is the steady state polarization calculated for the box model $\mathcal{P}_1^{ss}(N)\approx 0.92\sqrt{I+1}/\sqrt{NI}$.[30,31]

An important result of the calculations is that at the initial stage the DNSP dynamics can be well described by the box model. Note that this stage can be analytically modeled for an arbitrarily large number of nuclei with arbitrary spin I. Therefore the box model is an useful approximation for describing QDs, and is applicable up to the time when the curves for $n=1$ and $n=2$ in Fig. 3(a) start to deviate from each other. Similarly, the graded model with n nuclear groups is applicable as long as the curves for n and $n+1$ coincide.

The slow stage of DNSP development differs considerably with the step number. Generally it may be derived from the exact model with $n=N$. However, the computing time for this model with a macroscopic number of nuclei grows exponentially with N so that such calculations are impossible for real QDs. On the other hand, relaxation of the electron-nuclear spin system always occurs via, e. g., phonon baths or dipole-dipole interaction.[24] Therefore, our model, which does not consider relaxation, is applicable up to times shorter than the relaxation time. To describe the DNSP dynamics in this time range, the graded box model with $n\ll N$ can be exploited. For example, if the relaxation time corresponds to 50 time scale units in Fig. 3(a) the model with $n=3$ is sufficient. As the experiment shows, the characteristic spin relaxation time is of the order of milliseconds in (In,Ga)As/GaAs QDs.[32]

The electron-nuclear spin dynamics strongly depends on the excitation protocol. To illustrate this effect, we have done calculations for two cases: for the periodic excitation protocol and for a random one, which mimics continuous wave laser excitation. The results are compared to each other in Fig. 3(b). The DNSP develops slower for regular excitation.

The reason is that the electron spin polarization is partially restored toward the subsequent laser pulse due to the recurrence effect [see Fig. 2(b)], and therefore the efficiency of angular momentum transfer from electron to nuclei is reduced.

The recurrence effect for the electron-spin polarization has been predicted by Kozlov using the box model.[18] As seen from Fig. 2(b) the recurrence is also reproduced by the graded model and, therefore, is a characteristic feature of the coupled electron-nuclear spin system. For periodic excitation, the nuclei system is moved into a regular state which is characterized by a set of electron-spin precession frequencies. These frequencies depend on the distribution of the effective nuclear field. The distribution of its z projection, $W_z(B)=\langle\delta(B-\Sigma_k\mathcal{A}^{(k)}\hat{I}_z^{(k)}/\mu_B g_e)\rangle$, is shown in the inset of Fig. 3(b) for periodic and random excitation as well as without excitation. Initially, the distribution is related only to the NSF variation, which is almost Gaussian as predicted in Ref. 6. The Gaussian variance in typical QDs is about several tens of milliTesla,[33] which is orders of magnitude smaller than the maximal nuclear field, $B_N^{\max}=v_0\Sigma_j A_j|\psi(\mathbf{R}_j)|^2 I_j/\mu_B g_e$, for total nuclear polarization.[8] In our calculation, due to the relatively small number of nuclei, these quantities are, however, comparable. When pumping optically, the distribution is shifted due to the appearance of a regular nuclear field B_{Nz} and is narrowed due to a reduction of the NSF. Further, the statistics becomes modulated with an interval between the peaks, that is inversely proportional to the pulse repetition period ΔT.

IV. ELECTRON-NUCLEAR SPIN DYNAMICS UNDER MODULATED EXCITATION

Finally, we discuss how to qualitatively compare the model calculations with experiment. Two points should be stressed:

First, due to the limited number of nuclear spins, $N_{\text{model}}\sim 100$, considered in the model, only several tens of polarization pulses are needed to considerably change the nuclear spin state. At the same time, in real QDs containing $N_{\text{real}}\sim 10^5$ of nuclei, the number of excitation pulses required for obtaining the nuclear-spin polarization is $\gamma=N_{\text{real}}/N_{\text{model}}\sim 10^3$ times larger.

Second, tens or hundreds of nuclei taken into account are sufficient to let the electron spin "feel" the effect of the nuclear-spin bath. Indeed, the electron-spin dephasing in the field of NSF shown in Fig. 2(a) reproduces well the results obtained by Merkulov *et al.* (Ref. 6) for realistic QDs. However, a scaling parameter is needed to compare the calculated dynamics with experiment because the NSF field is approximately $\sqrt{\gamma}\sim 30$ times larger and, correspondingly, the dephasing time, τ_{deph}, is 30 times smaller in the model. In our calculations, we reduced the time interval between the excitation pulses ΔT proportionally, to get a ratio $\Delta T/\tau_{\text{deph}}\sim 10$ which is typical for the experiment.

These two effects due to the limited number of nuclear spins in the calculations gives rise only to a rescaling of the time axis for electron and nuclear spin dynamics, relative to the experimental observations. However, the dynamics of electron and nuclear-spin polarization should qualitatively reproduce those in realistic quantum dots.

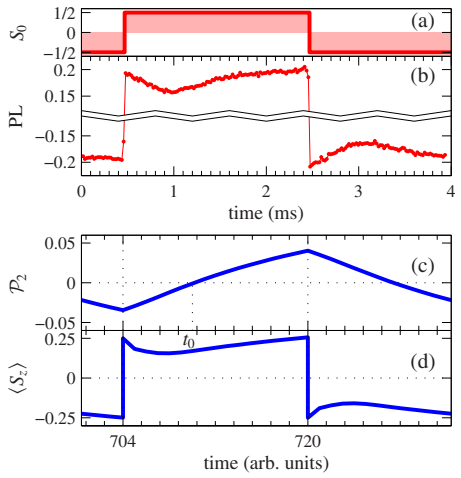

FIG. 4. (Color online) (a) Polarization dynamics protocol. The model QD contained 192 nuclei with spins $I=1/2$. $n=2$ steps have been used. (b) DNSP dynamics. (c) Dynamics of $\langle S_z\rangle$ at the moment of electron spin orientation. (d) Photoluminescence polarization from a corresponding experiment on (In,Ga)As/GaAs QDs.

To compare the theory developed with experiment, we discuss the electron-nuclear spin dynamics for the polarization modulation of excitation schematically shown in Fig. 4(a). The protocol has been used in experimental studies on (In,Ga)As/GaAs QDs, where the electron spin polarization has been detected through the polarization of the QD photoluminescence.[16] The modulation period used in the experiments was relatively small, so that the relaxation of nuclear spin polarization should not drastically modify the dynamics. The sample studied was annealed at 900 °C which considerably reduced the structural deformations of the QDs due to the InAs and GaAs lattice mismatch. Therefore, the quadrupolar splitting of nuclear spin states, recently discussed in Refs. 34 and 35, should not affect the dynamics in this case. Therefore, we can compare the experimental data with results of our modeling in which both the effects mentioned above have not been taken into account.

As seen in Fig. 4(b), each switching of the polarization helicity results in an instantaneous change in the electron spin polarization followed by a slow further evolution. This behavior can be explained by our model calculations in Figs. 4(c) and 4(d). The nuclear spins are slowly repolarized after each excitation polarization switching. At some time t_0 after switching, the DNSP becomes zero and the electron spin is affected by the nuclear spin fluctuations only. These fluctuations depolarize the electron spin efficiently, giving rise to the polarization dip. Its shift from t_0 is related to the modification of the NSF statistics discussed above.

V. SUMMARY

We have proposed an approach, the graded box model, for modeling the electron-nuclear spin dynamics in singly charged QDs under optical excitation. This model, applied for an increasing number of steps, reproduces the exact dy-

namics over an increasing time range. A periodic polarization protocol of the excitation gives rise to a coherent dynamics of the electron-nuclear spin system, which results in (a) a decreased rate of nuclear spin polarization and (b) a recurrence peak of the electron polarization after switching off the laser. The graded box model has been also applied to the analysis of an experimentally measured electron spin dynamics in (In,Ga)As/GaAs QDs for modulated excitation polarization. The good qualitative agreement with these data validates the graded box model.

ACKNOWLEDGMENTS

The authors thank I. Ya. Gerlovin for fruitful discussions. This work has been supported by the Russian Foundation for Basic Research, the Russian Ministry of Education and Science, and the Deutsche Forschungsgemeinschaft. M.Y.P. greatly acknowledges the Dynasty Foundation and the Government of St.-Petersburg.

APPENDIX: DIAGONALIZATION OF THE HAMILTONIAN MATRIX

To describe the matrix representation of the Hamiltonian (2), we can choose a set of basis functions

$$|\Upsilon\rangle = |S_z, J_1, L_1, J_2, L_2, \ldots, J_n, L_n, \beta\rangle. \tag{A1}$$

These functions have the following quantum numbers: $S_z = \pm 1/2$ is the electron spin z projection (in $\hbar$ units); J_k is the quantum number of the total angular momentum for kth group related to the mean angular momentum squared as $\langle \hat{\mathcal{I}}^2_{(k)} \rangle = J_k(J_k+1)$ (in $\hbar^2$ units); L_k denotes the quantum number of $\hat{\mathcal{I}}^{(k)}_z$ operator (in $\hbar$ units), respectively. Similar to the box model,[18] β is the set of all other quantum numbers needed for the state to be uniquely specified. The corresponding Hamiltonian matrix elements can be directly calculated as $H_{ij} = \langle \Upsilon_i | \hat{\mathcal{H}} | \Upsilon_j \rangle$, where i and j are the indexes of basis functions.

The Hamiltonian matrix can be represented in block-diagonal form with respect to set of total angular momenta $\mathcal{J} = \{J_1, J_2, \ldots, J_n\}$. The dimension of each such block (hereafter $\mathcal{J}$ block) equals to the number of possible combinations of z projections of the total nuclear angular momentum of each nuclear group multiplied by the number of possible projections of the electron spin: $2(2J_1+1)(2J_2+1)\ldots(2J_n+1)$.

The number of identical $\mathcal{J}$ blocks (with equal sets $\mathcal{J}$) equals to the product of functions $\Gamma_{\mathcal{N}_k}(J_k)$ which denote numbers of ways to obtain momentum J_k by summing of $\mathcal{N}_k$ elementary nuclear spins I. These functions are given by Eqs. (5a) and (5b) for particular elementary nuclear spins.

Each $\mathcal{J}$ block can be diagonalized independently. To illustrate general procedure, let us consider the model with two groups of nuclei. In this case we can consider a subset of basis functions with given $\mathcal{J} = \{J_1, J_2\}$ as $|S_z, L_1, L_2\rangle$. If this subset is sorted like

$$|\uparrow, J_1, J_2\rangle, |\downarrow, J_1, J_2\rangle, |\uparrow, J_1, J_2 - 1\rangle, \ldots, |\downarrow, J_1, -J_2\rangle,$$

$$|\uparrow, J_1 - 1, J_2\rangle, |\downarrow, J_1 - 1, J_2\rangle, \ldots, |\downarrow, J_1 - 1, -J_2\rangle, \ldots,$$

$$|\uparrow, -J_1, J_2\rangle, |\downarrow, -J_1, J_2\rangle, \ldots, |\downarrow, -J_1, -J_2\rangle,$$

then the matrix of $\mathcal{J}$ block, $H_{\mathcal{J}}$, has a block-tridiagonal form

$$H_{\mathcal{J}} = \begin{pmatrix} b_1 & c_1^T & & & \\ c_1 & b_2 & c_2^T & & \\ & c_2 & \ddots & \ddots & \\ & & \ddots & b_{p-1} & c_{p-1}^T \\ & & & c_{p-1} & b_p \end{pmatrix}. \tag{A2}$$

Here, $p = (2J_1+1)$ and dimension of each matrix b_k and c_k is $d = 2(2J_2+1)$. The matrices b_k are block-diagonal with blocks 1×1 and 2×2, and matrices c_k have only one nonzero diagonal above the principal diagonal.

The Hamiltonian matrix cannot be diagonalized analytically. However, we can apply a divide-and-conquer algorithm for block-tridiagonal matrices to obtain the eigenfunction expansion of the Hamiltonian numerically. The general idea of this method has been previously published in Ref. 27. If there are p diagonal subblocks of dimension d in $H_{\mathcal{J}}$, so it can be represented at the first step, *subdivision*, as a series of rank-d modifications of block-diagonal matrix B

$$H_{\mathcal{J}} = B + \sum_{i=1}^{p-1} W_i W_i^T, \tag{A3}$$

where $B = \text{block-diag}[\tilde{b}_1, \tilde{b}_2, \ldots, \tilde{b}_p]$. For this purpose, each off-diagonal subblock c_i should be first decomposed using singular value decomposition $c_i = U_i \Sigma_i V_i$, which can be found analytically for the graded box model. Then, the diagonal blocks can be written as

$$\tilde{b}_1 = b_1 - V_1 \Sigma_1 V_1^T, \tag{A4a}$$

$$\tilde{b}_i = b_i - U_{i-1}\Sigma_{i-1}U_{i-1}^T - V_i \Sigma_i V_i^T, \quad i = 2,3,\ldots,p-1, \tag{A4b}$$

$$\tilde{b}_p = b_p - U_{p-1}\Sigma_{p-1}U_{p-1}^T. \tag{A4c}$$

The matrices W_i in Eq. (A3) are given as

$$W_1 = \begin{pmatrix} V_1 \Sigma_1^{1/2} \\ U_1 \Sigma_1^{1/2} \\ 0 \\ 0 \end{pmatrix}, \quad W_{p-1} = \begin{pmatrix} 0 \\ 0 \\ V_{p-1}\Sigma_{p-1}^{1/2} \\ U_{p-1}\Sigma_{p-1}^{1/2} \end{pmatrix}, \tag{A5a}$$

$$W_i = \begin{pmatrix} 0 \\ V_i \Sigma_i^{1/2} \\ U_i \Sigma_i^{1/2} \\ 0 \end{pmatrix}, \quad i = 2,3,\ldots,p-2. \tag{A5b}$$

In the second step, *solution of subproblems*, one can diagonalize each $\tilde{b}_i$ matrix independently and then represent the problem as

$$H_{\mathcal{J}} = Q\left(D + \sum_{i=1}^{p-1} Y_i Y_i^T\right) Q^T, \tag{A6}$$

where $B=QDQ^T$ and $Y_i=Q^T W_i$. In the third step, *synthesis of the solutions of the subproblems*, one can find eigenvalues of the synthesis matrix $S=D+\Sigma_{i=1}^{p-1} Y_i Y_i^T$ by finding rank one modifications of diagonal matrix D.[27]

In the case of two groups of equivalent nuclei, the synthesis step involves a large number of eigenfunction expansions of 4×4 matrices, and, in principle, can be applied to a problem with very large number of nuclei. Calculations show that the algorithm described is rather effective because of the parallel character of the divide-and-conquer algorithm itself, which can be efficiently implemented using multiprocessor computers.

The described procedure can be also applied for models with $n>2$ groups in the same way. In this case, the matrix $H_{\mathcal{J}}$ is more cumbersome. However, the diagonal blocks b_i also have the block-tridiagonal form and, therefore, the divide-and-conquer algorithm should be applied recursively. Evidently, such a model requires more computational resources than the model with $n=2$ groups.

*m.yu.petrov@gmail.com

[1] *Spin Physics in Semiconductors*, edited by M. I. Dyakonov (Springer-Verlag, Berlin, 2008).

[2] *Semiconductor Quantum Bits*, edited by F. Henneberger and O. Benson (World Scientific, Singapore, 2009).

[3] *Semiconductor Spintronics and Quantum Computation*, edited by D. D. Awschalom, D. Loss, and N. Samarath (Springer-Verlag, Berlin, 2002).

[4] D. Gammon, Al. L. Efros, T. A. Kennedy, M. Rosen, D. S. Katzer, D. Park, S. W. Brown, V. L. Korenev, and I. A. Merkulov, Phys. Rev. Lett. **86**, 5176 (2001).

[5] A. V. Khaetskii, D. Loss, and L. Glazman, Phys. Rev. Lett. **88**, 186802 (2002).

[6] I. A. Merkulov, Al. L. Efros, and M. Rosen, Phys. Rev. B **65**, 205309 (2002).

[7] P.-F. Braun, X. Marie, L. Lombez, B. Urbaszek, T. Amand, P. Renucci, V. K. Kalevich, K. V. Kavokin, O. Krebs, P. Voisin, and Y. Masumoto, Phys. Rev. Lett. **94**, 116601 (2005).

[8] R. Oulton, A. Greilich, S. Yu. Verbin, R. V. Cherbunin, T. Auer, D. R. Yakovlev, M. Bayer, I. A. Merkulov, V. Stavarache, D. Reuter, and A. D. Wieck, Phys. Rev. Lett. **98**, 107401 (2007).

[9] J. Schliemann, A. V. Khaetskii, and D. Loss, Phys. Rev. B **66**, 245303 (2002).

[10] W. Zhang, V. V. Dobrovitski, K. A. Al-Hassanieh, E. Dagotto, and B. N. Harmon, Phys. Rev. B **74**, 205313 (2006).

[11] C. Deng and X. Hu, Phys. Rev. B **73**, 241303(R) (2006).

[12] L. M. Woods, T. L. Reinecke, and A. K. Rajagopal, Phys. Rev. B **77**, 073313 (2008).

[13] L. Cywiński, W. M. Witzel, and S. Das Sarma, Phys. Rev. Lett. **102**, 057601 (2009).

[14] A. Imamoğlu, E. Knill, L. Tian, and P. Zoller, Phys. Rev. Lett. **91**, 017402 (2003).

[15] H. Christ, J. I. Cirac, and G. Giedke, Phys. Rev. B **75**, 155324 (2007).

[16] R. V. Cherbunin, S. Yu. Verbin, T. Auer, D. R. Yakovlev, D. Reuter, A. D. Wieck, I. Ya. Gerlovin, I. V. Ignatiev, D. V. Vishnevsky, and M. Bayer, Phys. Rev. B **80**, 035326 (2009).

[17] S. M. Ryabchenko and Yu. Semenov, Sov. Phys. JETP **57**, 825 (1983) [Zh. Eksp. Teor. Fiz. **84**, 1419 (1983)].

[18] G. G. Kozlov, Sov. Phys. JETP **105**, 803 (2007) [Zh. Eksp. Teor. Fiz. **132**, 918 (2007)].

[19] A. I. Tartakovskii, T. Wright, A. Russell, V. I. Falko, A. B. Vankov, J. Skiba-Szymanska, I. Drouzas, R. S. Kolodka, M. S. Skolnick, P. W. Fry, A. Tahraoui, H.-Y. Liu, and M. Hopkinson, Phys. Rev. Lett. **98**, 026806 (2007).

[20] B. Urbaszek, P.-F. Braun, T. Amand, O. Krebs, T. Belhadj, A. Lemaítre, P. Voisin, and X. Marie, Phys. Rev. B **76**, 201301(R) (2007).

[21] A. V. Khaetskii and Y. V. Nazarov, Phys. Rev. B **61**, 12639 (2000).

[22] L. M. Woods, T. L. Reinecke, and Y. Lyanda-Geller, Phys. Rev. B **66**, 161318(R) (2002).

[23] M. Kroutvar, Y. Ducommun, D. Heiss, M. Bichler, D. Schuh, G. Abstreiter, and J. J. Finley, Nature (London) **432**, 81 (2004).

[24] *Optical Orientation*, edited by B. P. Zakharchenia and F. Meier (North-Holland, Amsterdam, 1984).

[25] To consider only the effect of inhomogeneous electron density, the hyperfine constants A_j for all the nuclei are taken to be equal.

[26] L. D. Landau and E. M. Lifshitz, *Quantum Mechanics: Nonrelativistic Theory* (Pergamon, Oxford, 1975).

[27] W. N. Gansterer, R. C. Ward, R. P. Muller, and W. A. Goddard, SIAM J. Sci. Comput. (USA) **25**, 65 (2003).

[28] A. Greilich, S. Spatzek, I. A. Yugova, I. A. Akimov, D. R. Yakovlev, Al. L. Efros, D. Reuter, A. D. Wieck, and M. Bayer, Phys. Rev. B **79**, 201305(R) (2009).

[29] Spin $I=1/2$ has been chosen here to reduce the computation time.

[30] G. G. Kozlov, arXiv:0801.1391 (unpublished).

[31] M. Yu. Petrov, G. G. Kozlov, and I. V. Ignatiev, *Proceedings of the 16th International Symposium on Nanostructures: Physics and Technology*, (A. F. Ioffe Physico Technical Institute, St.-Petersburg, 2008) p. 226.

[32] P. Maletinsky, A. Badolato, and A. Imamoglu, Phys. Rev. Lett. **99**, 056804 (2007).

[33] M. Yu. Petrov, I. V. Ignatiev, S. V. Poltavtsev, A. Greilich, A. Bauschulte, D. R. Yakovlev, and M. Bayer, Phys. Rev. B **78**, 045315 (2008).

[34] R. I. Dzhioev and V. L. Korenev, Phys. Rev. Lett. **99**, 037401 (2007).

[35] P. Maletinsky, M. Kroner, and A. Imamoglu, Nat. Phys. **5**, 407 (2009).